



Identification of nanofiltration fouling layer constituents

Florencia Saravia*, Angela Klüpfel, Amadeu Zamora Richard, Fritz H. Frimmel

Karlsruhe Institute of Technology (KIT), Engler-Bunte-Institut, Water Chemistry and Water Technology,

Engler-Bunte-Ring 1, 76131, Karlsruhe, Germany

Tel. +49 721 608 42593; Fax: +49 721 47051; email: florencia.saravia@kit.edu

Received 15 October 2012; Accepted 8 February 2013

ABSTRACT

Application of nanofiltration (NF) membranes has increased during the last years: many industries from drinking water treatment and water re-use to the pharmaceutical and food industry deal with the application of NF and its drawbacks. One of the main problems of membrane technology is fouling. Fouling during NF is a complex problem because of the importance of the membrane surface properties (e.g. charge and structure) and the corresponding interactions between the water constituents and the membrane. In this work, the fouling layer composition of three membranes was investigated using different raw waters and it was correlated with the membrane performance. Rejection properties depended to a great extent on the water composition and the ionic strength of the raw water. Investigations of fouling layer compositions suggest that the membrane properties play a key role for flux decline and the related “amount” of fouling material on the membranes and its constituents.

Keywords: Nanofiltration; Fouling; Cations; NOM-membrane interactions

1. Introduction

Nanofiltration (NF) is a relatively young membrane technique that has gained importance in many applications during the last decade, reaching from drinking water treatment and wastewater reclamation to manifold industrial applications. Sometimes the implementation of NF is limited because of fouling formation and the corresponding decline of permeability, leading to enhanced operational costs and a reduction of the membrane's lifetime. In various publications, membrane fouling has been related to feed water chemistry, operating conditions and membrane surface properties [1–5].

Membrane surface roughness was found to be strongly correlated with fouling in studies performed

by Zhu and Elimelech [3], Elimelech et al. [1] and Vrijenhoek et al. [2]. Cho et al. [6] and Boussu et al. [7] found that a high negative zeta potential of the membrane minimized fouling, whereas the influence of the membrane's hydrophobicity depended on the feed water composition. In AFM (atomic force microscopy) experiments, Yamamura et al. [8] found a positive correlation between natural organic matter (NOM) adsorption, as well as the amount of foulant functional groups and membrane blockage. Concerning the operating conditions, a low permeation drag (controlled by permeate flux) and a high crossflow velocity decreased fouling in studies conducted by Zhu and Elimelech [3], Amy and Cho [9] and Seidel and Elimelech [10]. In addition, several raw water properties have been proven to significantly influence fouling formation. Generally, the

*Corresponding author.

presence of divalent cations, especially Ca^{2+} [4,9–16], the increase in ionic strength [4,9,11,15–17] and lower [11,17] or higher pH-value [14] were shown to enhance NOM fouling due to charge interactions between membrane and NOM functional groups as well as changes in NOM configuration. Ahn et al. [4] investigated the addition of different cations at the same ionic strength and found that fouling increased in the order $\text{Ca}^{2+} > \text{Mg}^{2+} > \text{Na}^+$. Autopsy tests performed by Gwon et al. [18] revealed inorganically bound Ca^{2+} and organically bound Si as major foulants and Fe as main contributor to irreversible fouling of the membrane after filtration of groundwater. Furthermore, the properties of organic water constituents were found to have a strong influence on their tendency to accumulate on the membrane surface [12,19,20]. Intensive fouling characterization with ^{13}C NMR and Fourier transform infrared spectroscopy (FTIR) by Frimmel et al. [21] and Her et al. [5] showed that protein- and polysaccharide-like substances play a major role in organic fouling during filtration of natural waters.

Based on their experimental results, Lin et al. [22] quantified the amount of dissolved organic matter (DOM) deposited on ultrafiltration (UF) membranes and proposed two classes of fouling schemes. For a denser UF membrane (molecular weight cut-off MWCO=10 kDa), DOM was assumed to cause flux decline by binding or aggregation and, hence by formation of a surface gel layer, whereas a loose UF membrane (MWCO=100 kDa) was assumed to be fouled by inner pore adsorption and pore blockage. For NF, similar information is missing. Therefore, quantitative information about the identity and localization of membrane foulants will help to enhance the understanding of fouling mechanisms and to improve pre-treatment methods and operating parameters with the objective of increasing the membrane's lifetime.

The aim of this study was to identify the fouling constituents after NF of a soft and NOM-rich water with and without addition of multivalent ions at different concentrations. More precisely, the substances deposited on the membrane surface on the one hand and in the membrane pores on the other hand should be distinguished and quantified. Therefore, batch experiments were conducted in a bench-scale cross-flow plant. Six flat-sheet modules were equipped with three different membranes (each one in duplicate). After filtration of a defined permeate volume per module, parts of the fouling layers (FL) were scraped of the membranes and both FL and membranes were analysed concerning deposited organic carbon (OC) and ions. Additionally, the structure and properties of the FL and membranes were characterized using

scanning electron microscopy (SEM), attenuated total reflection Fourier transform infrared spectroscopy (ATR-FTIR) and contact angle measurements to quantify hydrophobicity.

2. Materials and methods

Experiments were carried out with a crossflow membrane set-up consisting of six flat-sheet units equipped with three membranes (NF200, Polypiperazine, Dow Filmtech, MWCO=200 Da, Desal HL, PA, Osmonics, MWCO=190 Da and P005F, PES, Nadir, MWCO=1,400 Da). During the experiments the temperature was maintained at $25 \pm 0.5^\circ\text{C}$, and the transmembrane pressure was set at 5 bar. Before the experiments, deionized (DI) water was filtered through the membranes for 24 h for elimination of water-soluble organic substances in the membrane structure. Membrane molecular weight cut-off was determined with the crossflow set-up (filtration condition: 5 bar and 25°C) using different saccharides and polyethyleneglycols (PEG).

The raw water used in this work was soft and NOM-rich (Lake Hohloh, Black Forest, Germany, sample nr. 22, HO22). Table 1 shows the main properties of the water matrix.

Before the experiments, the water matrix was $0.45\ \mu\text{m}$ filtered in order to eliminate particulate substances and diluted with ID-water to a DOC-concentration of approximately 5.5 mg/L. Experiments were carried out by adding different cations (calcium and iron as CaCl_2 and FeCl_3 , Merck, Germany) and anions (sulphate, phosphate as sodium salts, Merck, Germany) at different concentrations to the NOM-rich water. The pH-value of the feed solutions was adjusted to 7.5 ± 0.2 with NaOH. Additionally, NaN_3 (4 mg/L, Merck, Germany) was added to the feed water to inhibit bacterial growth. All experiments were performed in duplicate.

The structure and properties of FL and membranes were characterized using SEM (scanning electron microscopy, LEO 1530, Gemini), ATR-FTIR spectroscopy (attenuated total reflection Fourier transform infrared, IFS 55, EQUINOX, Bruker optics, Germany), Z-potential (EKA, Anton Paar, Austria) and contact angle (hydrophobicity) measurements (OCA10, Dataphysics, Germany). Additionally, the OC-concentration, cation and anion concentrations in the FL and in the membrane "pores" were measured. Distinction between pore and surface fouling was conducted mechanically applying the method proposed by Gorenflo et al. [23]. The method consists of fixing the membrane on a flat surface between two virgin and wet membrane pieces. The fouling layer is removed

Table 1
Properties of the raw water matrix (Lake Hohloh, HO22, 0.45 μm filtered)

pH (12 °C)	El. cond. (16 °C) ($\mu\text{S}/\text{cm}$)	DOC (mg/L)	UVA (254 nm) (m^{-1})	VIS (254 nm) (m^{-1})	Ca^{2+} ($\mu\text{g}/\text{L}$)	Na^+ ($\mu\text{g}/\text{L}$)	Cl^- (mg/L)	SO_4^{2-} (mg/L)
4.5	27.8	29.8	148	15.5	405	446	1.38	2.07

using a polyvinylidene fluoride (PVDF) slide. The presence of the new membranes on both sides of the fouled membrane served as spacers that prevented the damage of the fouled membrane by the slide. For OC-determination, FL were dissolved in 0.01 M NaOH. For the measurement of cations and/or anions, FL were added to a HCl solution (0.01 M) for 12 h, and the cation concentrations were measured in the supernatant solution. A similar procedure was performed with the membrane after fouling layer removal: one piece of membrane with “pore fouling” was submerged for 12 h in NaOH (0.01 M) and a second piece of membrane was submerged for 12 h in HCl (0.01 M). In the supernatant solution belonging to the first piece of membrane, OC was measured, and in the supernatant solution belonging to the second piece of membrane, the cation and/or anion concentrations were determined. OC, cation and anion concentrations for the FL and for the pores are reported as mg (DOC/ions) per permeate volume (in L), per m^2 membrane surface, within this article.

During the experiments, typical parameters such as feed and permeate flow, pressure, temperature and TOC (total organic carbon)/ions removal were measured. The TOC concentration was measured with the TOC-Analyzer, Model 800 (Sievers Instruments, USA). Cation concentrations of feed and permeate samples were measured with a ICP-OES (Inductively Coupled Plasma Optical Emission Spectroscopy) spectrometer (Varian, Vista PRO CCD). A Dionex ion chromatography system (DX 500, Dionex) was used to determine the phosphate and sulphate concentrations.

For further characterization of the NOM removal, LC-UV/OCD chromatograms of feeds and permeates were measured. LC-UV/OCD measurements were carried out using a TSK-HW-50S column. A phosphate buffer (0.028 mol/L) at pH=6.8 was used as eluent. The flow rate was set at 1 mL/min [24].

3. Results and discussion

3.1. NOM removal

NOM-removal represents the percentage of NOM in raw water eliminated by the membrane and was calculated from the TOC-values in raw water and

permeates. During the experiments, the NOM-removal was: 95–99% for NF200, 91–99% for Desal HL and 85–96% for P005 F. In almost all experiments, a light increase in NOM-removal (max. 3%) with increasing filtration time was observed, probably due to fouling formation.

All LC-OCD chromatograms of the experiments showed a similar trend, independent on the ion concentration in the raw water. As an example, Fig. 1 shows the LC-OCD chromatograms of raw water and permeates for the experiment with a calcium concentration of 40 mg/L. NF200 and Desal HL presented similar removal properties: the high molecular weight fraction, also called biopolymer fraction, containing polysaccharide and polysaccharide-like substances [25], retention time, t_r , between 25 and 32 min) and the humic fraction (between 32 and 50 min) were completely removed after filtration. The last fraction (retention time > 50 min), containing hydrophobic structures and low molecular weight organic acids [24] was eliminated to more than 93% by the NF-membranes. In the permeate of P005, it can be observed that parts of the humic acid fraction and the low molecular weight/hydrophobic fraction remained in the permeate. P005F has a higher MWCO and, hence, less organic material can be retained by the membrane. Furthermore, it must be taken into consideration that during membrane filtration apart from size exclusion several other effects affect the rejection

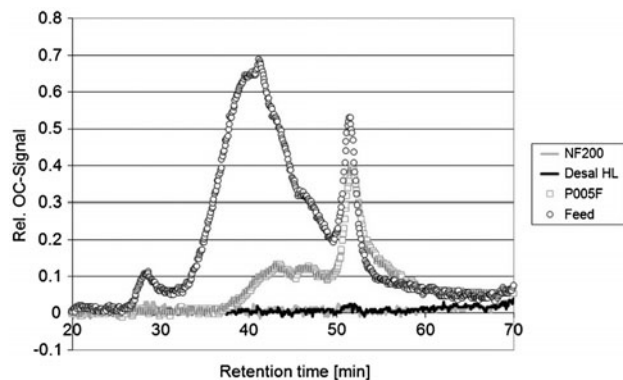


Fig. 1. LC-OCD chromatogram of raw water and permeates (NF200, Desal HL and P005F). Experiment with $\rho(\text{Ca}^{2+}) = 40 \text{ mg}/\text{L}$.

properties of membranes. The organic substances contained in the feed can interact with the membrane and accumulate on its surface or pores altering the separation properties and achieving rejection rates which do not directly relate to the nominal size of the membrane pores [15,26].

3.2. Ion removal

Filtration experiments using calcium as model ion for divalent cations showed that with increasing calcium concentration in the feed all membranes presented an increase of calcium in the permeate (Fig. 2). The decline of calcium removal can be explained by the Donnan effect [10]. In addition, calcium causes a shielding effect on the negatively charged membrane [27] and therefore changes the electrostatic interaction of the membrane surface and charged water constituents. The Ca^{2+} -rejection in the experiments with the “mix” solution showed for all membranes a higher rejection rate than it was seen in experiments with similar Ca^{2+} -concentration were calcium was only added as CaCl_2 . In the experiments with “only” calcium, the electro neutrality of the permeate solution can be achieved only if Ca^{2+} -ions flow through the membrane in order to compensate the charge of the small, monovalent Cl^- -ions. Therefore, the calcium concentration in the permeate increases (resulting in a decreasing Ca^{2+} -removal rate). In the experiments with the “mix”-solution, Na^+ -ions are available to compensate the anions in the permeate and the calcium concentration in the permeate decreases (increasing the Ca^{2+} -removal rate). A similar trend was observed by increasing sulphate concentration in the feed.

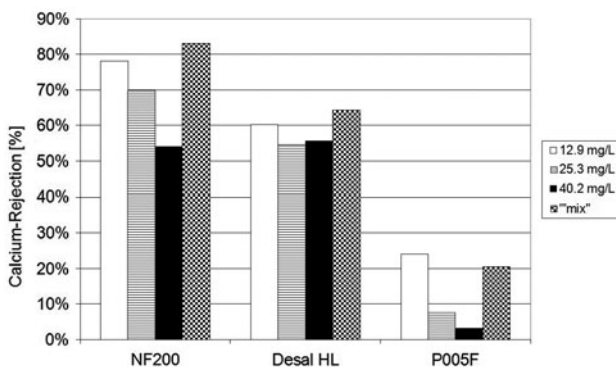


Fig. 2. Calcium rejection (%) by NF200, Desal HL and P005F. Experiments with different calcium concentrations ($\rho(\text{Ca}^{2+}) = 12.9, 25.3, 40.2 \text{ mg/L}$) and a mix of salts ($\rho(\text{Ca}^{2+}) = 24.3 \text{ mg/L}$ as CaCl_2 , $\rho(\text{Fe}^{3+}) = 0.19 \text{ mg/L}$ as FeCl_3 , $\rho(\text{SO}_4^{2-}) = 28.7 \text{ mg/L}$ as Na_2SO_4).

Due to their high hydration diameter and the size of the ions, iron and phosphate removal rates were very high (>97%).

3.3. Permeability

The membrane flux during filtration remained relatively constant for NF200 and Desal HL with a maximum decrease of 90 and 83%, respectively, after 5,000 L permeate per m^2 membrane surface, compared with the initial fluxes J_0 . An influence of water composition on flux decline could be clearly seen for P005F (Fig. 3). For this membrane, flux decline was stronger and increased with increasing raw water concentration of calcium.

The denser membranes NF200 and Desal HL showed similar MWCOs (200 and 190 Da, respectively) and similar intrinsic resistances (4.4 and $3.7 \times 10^{13} \text{ 1/m}$, respectively). P005F, in contrast, had a higher MWCO and a resistance of $2.8 \times 10^{13} \text{ 1/m}$. Since the experiments were performed at a fixed transmembrane pressure, the lower resistance led to an enhanced permeate drag for P005F and, consequently, to a higher ratio J_0/k (k : mass transfer coefficient from the concentration polarization layer [28]). The higher convective flow to the membrane surface may result in an increased deposition of water constituents on the membrane and in a compaction of the fouling layer. Additionally, a higher MWCO may enhance the membrane's sensitivity to pore blocking as will be shown later.

3.4. Fouling characterization

3.4.1. Organic fouling

For all the investigated membranes it was observed that

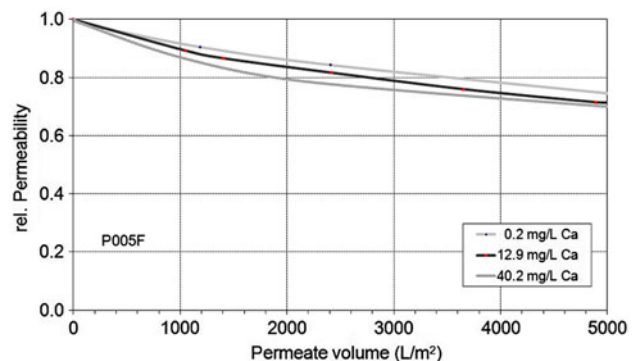


Fig. 3. Permeability decline in the experiments with the membrane P005F.

- a higher flux decline was correlated with a higher amount of organic deposits and
- a higher calcium concentration in the feed resulted in a higher accumulation of NOM at the membrane surface.

The latter was found to be especially pronounced in the experiments with Desal HL, where the OC-concentration in the fouling layer grew from 1.6 mg per permeate volume (in L), per m² membrane surface with no addition of calcium to 7.5 mg/L m² with 12.9 mg/L calcium addition (Fig. 4).

SEM-pictures of the membrane showed a similar trend than the OC-concentrations on membrane surface (see Fig. 5, cross section of the FL). On the NF200 Membrane, a very thin fouling layer was observed (see also Fig. 6), whereas in the Desal HL and the P005, thicker FL were found.

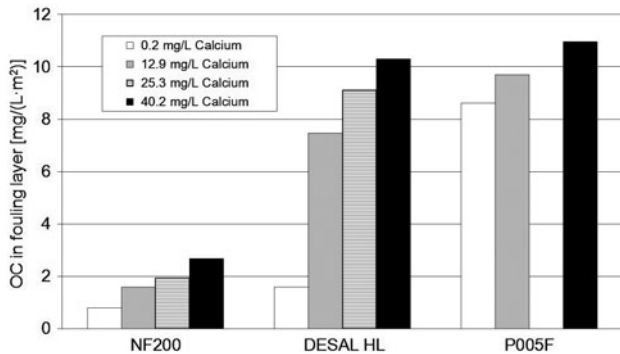


Fig. 4. OC-concentration in the surface FL of different NF-membranes after filtration of NOM-rich water. The calcium concentration in the raw water was adjusted by addition of CaCl₂.

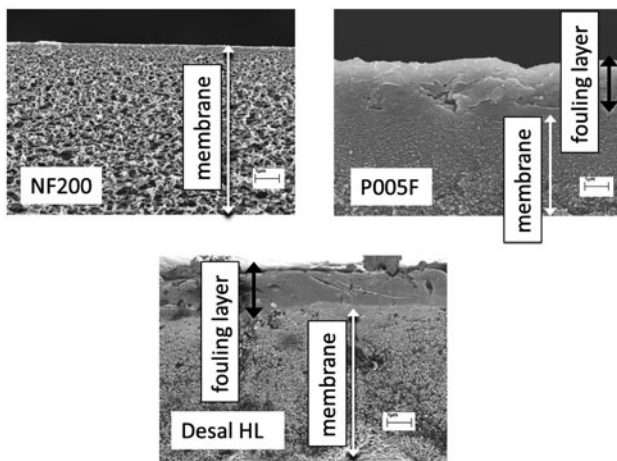


Fig. 5. SEM-pictures (cross-section) of the FL after filtration. Experiment with $\rho(\text{Ca}^{2+}) = 0.2 \text{ mg/L}$.

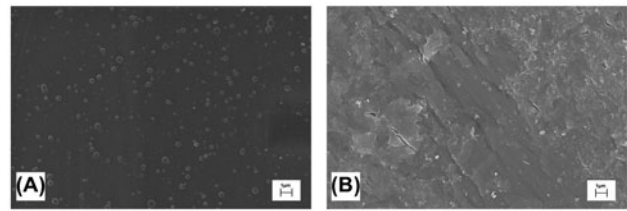


Fig. 6. SEM-pictures of the FL on the NF200 surface after filtration. Experiment with $\rho(\text{Ca}^{2+}) = 0.2 \text{ mg/L}$. A: virgin membrane, B: fouled membrane.

Considering the different properties of the membranes used, P005F presents a Z-potential of approx. 0 mV at a pH value of 7, while at this pH, NF200 and Desal HL show Z-potentials of approximately. -17 and -18 mV [2], respectively. Membranes with low Z-potential may exhibit less NOM-fouling because of higher electrostatic repulsion between membrane surface and negatively charged NOM-molecules. In the experiments, Z-potential values and membrane resistance corresponded with a high deposition rate of NOM with and without Ca-addition for P005F. The differences in the influence of calcium between NF200 and Desal HL can be related to other surface parameters such as roughness [2]. The OC-concentration in the membrane pores was below the limit of detection of the TOC-measurement system (0.1 mg/L).

Table 2 shows the contact angle measurements of the membranes. NF200 was clearly the most hydrophilic membrane, and thus, there was a minimal accumulation of hydrophobic organic substances. Desal HL and P005 present higher contact angle values, corresponding to less hydrophilic surfaces. Additionally, for P005F, the difference between advancing and receding contact angle (contact angle hysteresis) is relatively high. Wenzel [29], Adam [30] and many others authors showed that the roughness influences the contact angle measurement. Cassie and Baxter [31], Chen et al. [32] and Extrand [33] presented in their works that the difference between advancing and receding contact angle depends first on the molecular interactions between the liquid and the surface, and second

Table 2
Contact angle of the applied membranes ($n = 12$)

Membrane	NF200	Desal HL	P005F
θ_a (standard deviation)	7.2° (2.1)	26.3° (2.3)	66.0° (1.8)
θ_r (standard deviation)	5° (2.2)	16.1° (2.3)	26.5° (1.1)
$\Delta\theta$ (contact angle hysteresis)	2°	10.2°	39.5°

on the surface properties (principally the roughness) of the surface. Small differences ($<5^\circ$) between advancing and receding angles suggest that the surface is smooth. The membranes (Desal HL and P005F) with higher contact angles (more hydrophobic) and higher contact angle hysteresis (higher roughness) presented the highest OC accumulation on their surfaces.

Apart from the adsorption bands corresponding to the original membrane material, the ATR-FTIR spectra of the fouled membranes clearly exhibited two additional bands at 916–918 and 1,032 cm^{-1} , which correspond to carbohydrates or carbohydrate like substances [34]. The results confirm that polysaccharide like substances are a principal component of FL [6,21].

Additional bands corresponding to the fouling layer were interfered by the strong signals of the virgin membrane. Fig. 7 shows the spectra of virgin and fouled NF200 samples. The typical adsorption bands at around 1,592 and 1,110 cm^{-1} (aromatic double bonded carbons), at 1,492 cm^{-1} (methyl groups), at 1,016 cm^{-1} (ether groups), at 1,151 and 694 cm^{-1} (sulphone groups) correspond to the membrane support material (PS) [14].

3.4.2. Ions in surface and pore fouling

Measurement of ion-concentration showed a constant concentration of calcium in the pores of NF-200 and an almost constant concentration in case of Desal HL independent of the Ca-concentration in the raw water (see Fig. 8), but an increasing amount in the fouling layer with higher Ca-concentration in the feed (see Fig. 9).

Like for OC, the amount of Ca in the P005F surface FL was not significantly higher in comparison with the other membranes. However, P005F showed a considerably higher amount of calcium in the membrane

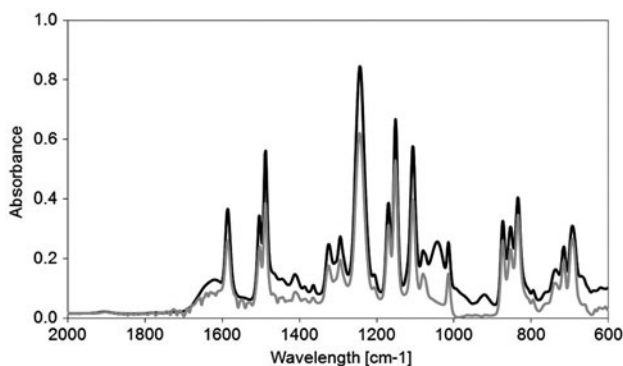


Fig. 7. ATR-FTIR spectra of a virgin NF200 membrane (in grey) and a fouled NF200 membrane (in black).

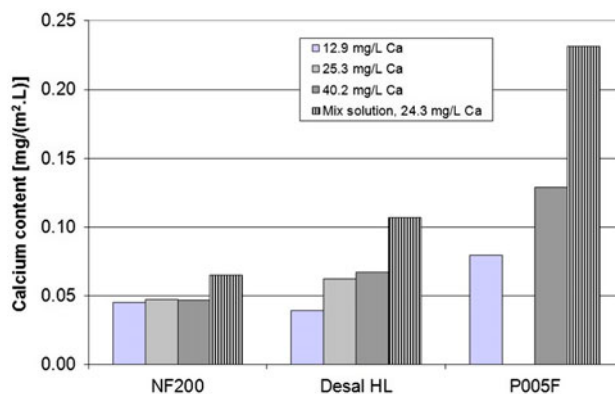


Fig. 8. Calcium content in the pores of different NF-membranes after filtration of NOM-rich water. The calcium concentrations in the raw water were adjusted by addition of CaCl_2 . Mix solution: $\rho(\text{Ca}^{2+}) = 24.3 \text{ mg/L}$ as CaCl_2 , $\rho(\text{Fe}^{3+}) = 0.19 \text{ mg/L}$ as FeCl_3 , $\rho(\text{SO}_4^{2-}) = 28.7 \text{ mg/L}$ as Na_2SO_4 .

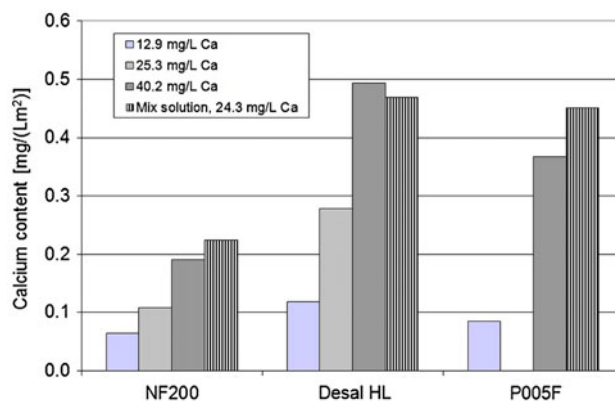


Fig. 9. Calcium content in the surface FL of different NF-membranes after filtration of NOM-rich water. Calcium concentration in the raw water was adjusted by addition of CaCl_2 . $\rho(\text{Ca}^{2+}) = 24.3 \text{ mg/L}$ as CaCl_2 , $\rho(\text{Fe}^{3+}) = 0.19 \text{ mg/L}$ as FeCl_3 , $\rho(\text{SO}_4^{2-}) = 28.7 \text{ mg/L}$ as Na_2SO_4 .

structure for all experiments. This supports the hypothesis that the stronger flux decline of P005F and its more distinctive sensitivity to the raw water calcium concentration can be attributed to pore-blocking phenomena caused by its higher MWCO.

It can be suggested that in the “pores” or polymer matrix of the tight NF-membranes calcium may adsorb (as cation) or accumulate (as a complex with NOM) achieving a maximal amount, which depends on pore-size, shape and charge. In the FL, as expected, the amount of calcium increased with increasing OC deposited on the membrane surface.

For P005 F and Desal HL, the ratios of calcium and OC amount in the FL were similar and the ratios

of $\text{Ca}^{2+}(\text{FL})/\text{OC}(\text{FL})/\rho(\text{Ca}^{2+}\text{RW})$ were constant for different calcium raw water concentrations. For NF200, the ratios of calcium and OC amount in the FL were higher and the ratios of $\text{Ca}^{2+}(\text{FL})/\text{OC}(\text{FL})/\rho(\text{Ca}^{2+}\text{RW})$ decreased with increasing calcium concentration in the raw water. Hence, calcium was present mainly in form of Ca–OC complexes in the case of P005F and Desal HL FL, but not only as Ca–OC complex in the case of NF200. For NF200, the calcium concentration in the gel layer just upon the membrane surface seems to be higher than for P005F and Desal HL at low calcium raw water concentrations. This effect becomes smaller at higher raw water concentrations due to shielding effects.

In the experiments with the mix solution the Ca-content in the fouling layer was significantly higher compared to the experiments with addition of CaCl_2 . Calcium removal rates in the experiments with the mix solution were relatively high. In combination with the low-solubility products of CaSO_4 and $\text{Fe}(\text{OH})_3$, this lead to an increased deposition of calcium (and Fe) in the surface fouling layer. This effect was even more pronounced for the accumulation of ions within the membrane structure.

4. Conclusions

Fouling formation is generally influenced by the raw water characteristics, membrane properties and the filtration procedure. The amount of fouling (measured as mg OC per m^2 membrane surface and L permeate volume) correlates with the membrane properties: membranes with a low (negative) Z-potential and a high intrinsic resistance (NF200 and Desal HL) showed a lower amount of fouling layer on their surface and a more stable permeate flux in comparison to experiments with no addition of salts. In the experiment with addition of calcium, an increase in fouling layer mass and an increasing flux decline were observed. Calcium obviously forms complexes with NOM and at the same time shields the negatively charged membrane surface causing a higher deposition of NOM on the membrane surface. The concentrations of calcium and iron in the FL correlated for NF200 and P005F with the Z-potential of the membranes as well: in the FL of P005F (neutral at $\text{pH}=7$) high calcium and iron concentrations were detected. Unexpectedly, high calcium and iron concentrations (data not shown) were found in the FL of Desal HL. In this case, the high calcium and iron concentrations went along with an increase in OC on the membrane surface. This membrane charge seems to be shielded by the addition of salts to a greater extent than NF200. Differences in the performance of NF-200 and

Desal HL can be explained by different surface roughness and/or surface treatments.

The concentration of ions in the membrane “pores” correlated directly with the MWCO of the membranes.

However, the organic constituents of the FL were independent of membrane material and/or their properties. Polysaccharides were generally recognized by ATR-FTIR as major foulants in all investigated membranes irrespective of the membrane material or properties.

Acknowledgements

The authors would like to thank the German Technical and Scientific Association for Gas and Water (DVGW), Bonn, the German Water Chemical Society for a PhD grant and the German Ministry of Education & Research (BMBF), SMART II research project (Ref. 02WM1079), for financial support.

References

- [1] M. Elimelech, Z. Xiaohua, A.E. Childress, H. Seungkwan, Role of membrane surface morphology in colloidal fouling of cellulose acetate and composite aromatic polyamide reverse osmosis membranes, *J. Membr. Sci.* 127 (1997) 101–109.
- [2] E.M. Vrijenhoek, S. Hong, M. Elimelech, Influence of membrane surface properties on initial rate of colloidal fouling of reverse osmosis and nanofiltration membranes, *J. Membr. Sci.* 188 (2001) 115–128.
- [3] X. Zhu, M. Elimelech, Colloidal fouling of reverse osmosis membranes: measurements and fouling mechanisms, *Environ. Sci. Technol.* 31 (1997) 3654–3662.
- [4] W.-Y. Ahn, A.G. Kalinichev, M.M. Clark, Effects of background cations on the fouling of polyethersulfone membranes by natural organic matter: experimental and molecular modeling study, *J. Membr. Sci.* 309 (2008) 128–140.
- [5] N. Her, G. Amy, A. Plottu-Pecheux, Y. Yoon, Identification of nanofiltration membrane foulants, *Water Res.* 41 (2007) 3936–3947.
- [6] J. Cho, G. Amy, J. Pellegrino, Y. Yoon, Characterization of clean and natural organic matter (NOM) fouled NF and UF membranes, and foulants characterization, *Desalination* 118 (1998) 101–108.
- [7] K. Boussu, C. Vandecasteele, B. Van der Bruggen, Relation between membrane characteristics and performance in nanofiltration, *J. Membr. Sci.* 310 (2008) 51–65.
- [8] H. Yamamura, K. Kimura, T. Okajima, H. Tokumoto, Y. Watanabe, Affinity of functional groups for membrane surfaces: implications for physically irreversible fouling, *Environ. Sci. Technol.* 42 (2008) 5310–5315.
- [9] G. Amy, J. Cho, Interactions between natural organic matter (NOM) and membranes: rejection and fouling, *Water Sci. Technol.* 40 (1999) 131–139.
- [10] A. Seidel, M. Elimelech, Coupling between chemical and physical interactions in natural organic matter (NOM) fouling of nanofiltration membranes: implications for fouling control, *J. Membr. Sci.* 203 (2002) 245–255.
- [11] S. Hong, M. Elimelech, Chemical and physical aspects of natural organic matter (NOM) fouling of nanofiltration membranes, *J. Membr. Sci.* 132 (1997) 159–181.
- [12] A.I. Schäfer, A.G. Fane, T.D. Waite, Nanofiltration of natural organic matter: removal, fouling and the influence of multivalent ions, *Desalination* 118 (1998) 109–122.

- [13] S.-H. Yoon, C.-H. Lee, K.-J. Kim, A.G. Fane, Effect of calcium ion on the fouling of nanofilter by humic acid in drinking water production, *Water Res.* 32 (1998) 2180–2186.
- [14] N. Her, G. Amy, C. Jarusutthirak, Seasonal variations of nanofiltration (NF) foulants: identification and control, *Desalination* 132 (2000) 143–160.
- [15] F. Saravia, C. Zwiener, F.H. Frimmel, Interactions between membrane surface, dissolved organic substances and ions in submerged membrane filtration, *Desalination* 192 (2006) 280–287.
- [16] C. Jarusutthirak, S. Mattaraj, R. Jiratananon, Influence of inorganic scalants and natural organic matter on nanofiltration membrane fouling, *J. Membr. Sci.* 287 (2007) 138–145.
- [17] A. Braghetta, F.A. DiGiano, W.P. Ball, NOM accumulation at NF membrane surface: impact of chemistry and shear, *J. Environ. Eng.* 124 (1998) 1087–1098.
- [18] E.-M. Gwon, M.-J. Yu, H.-K. Oh, Y.-H. Ylee, Fouling characteristics of NF and RO operated for removal of dissolved matter from groundwater, *Water Res.* 37 (2003) 2989–2997.
- [19] B. Van der Bruggen, L. Braeken, C. Vandecasteele, Evaluation of parameters describing flux decline in nanofiltration of aqueous solutions containing organic compounds, *Desalination* 147 (2002) 281–288.
- [20] A.E. Contreras, A. Kim, Q. Li, Combined fouling of nanofiltration membranes: mechanisms and effect of organic matter, *J. Membr. Sci.* 327 (2009) 87–95.
- [21] F.H. Frimmel, F. Saravia, A. Gorenflo, NOM removal from different raw waters by membrane filtration, *Water Sci. Technol.: Water Suppl.* 4 (2004) 165–174.
- [22] C.-F. Lin, A. Yu-Chen Lin, P. Sri Chandana, C.-Y. Tsai, Effects of mass retention of dissolved organic matter and membrane pore size on membrane fouling and flux decline, *Water Res.* 43 (2009) 389–394.
- [23] A. Gorenflo, S. Eker, F.H. Frimmel, Surface and pore fouling of flat sheet nanofiltration and ultrafiltration membranes by NOM, in: *International Conference on Membrane Technology for Waste Water Reclamation and Reuse*, Israel, 2001, pp. 127–140.
- [24] S.A. Huber, F.H. Frimmel, Size-exclusion chromatography with organic carbon detection (LC-OCD). A fast and reliable method for the characterization of hydrophilic organic matter in natural waters, *Vom Wasser* 86 (1996) 277–290.
- [25] S.A. Huber, A. Balz, M. Abert, W. Pronk, Characterisation of aquatic humic and non-humic matter with size-exclusion chromatography-organic carbon detection-organic nitrogen detection (LC-OCD-OND), *Water Res.* 45 (2011) 879–885.
- [26] M.B. Müller, W. Fritz, U. Lankes, F.H. Frimmel, Ultrafiltration of nonionic surfactants and dissolved organic matter, *Environ. Sci. Technol.* 38 (2004) 1124–1132.
- [27] J.M.M. Peeters, J.P. Boom, M.H.V. Mulder, H. Strathmann, Retention measurements of nanofiltration membranes with electrolyte solutions, *J. Membr. Sci.* 145 (1998) 199–209.
- [28] S. Lee, J. Moon, S.-K. Yim, S.-H. Moon, J. Cho, The relationship between flux decline of NF membranes with NOM transport characteristics: convection vs. diffusion, *Desalination* 147 (2002) 237–241.
- [29] R.N. Wenzel, Resistance of solid surfaces to wetting by water, *J. Indus. Eng. Chem.* 28 (1936) 988–994.
- [30] N.K. Adam, *Physics and Chemistry of Surfaces*, third ed., Oxford University Press, London, 1949.
- [31] A.B.D. Cassie, S. Baxter, Wettability of porous surfaces, *Trans. Faraday Soc.* 40 (1944) 546–551.
- [32] W. Chen, A.Y. Fadeev, M.C. Hsieh, D. Oner, J. Youngblood, T.J. McCarthy, Ultrahydrophobic and ultralyophobic surfaces: some comments and examples, *Langmuir* 15 (1999) 3395–3399.
- [33] C.W. Extrand, Model for contact angles and hysteresis on rough and ultraphobic surfaces, *Langmuir* 18 (2002) 7991–7999.
- [34] J.P. Croué, M.F. Benedetti, D. Violleau, J.A. Leenheer, Characterization and copper binding of humic and nonhumic organic matter isolated from the south Platte river: evidence for the presence of nitrogenous binding site, *Environ. Sci. Technol.* 37 (2002) 328–336.